Analysis of a Bladed Disk with Friction in Blade Attachments

Damien Charleux, Claude Gibert, Fabrice Thouverez, Jean-Pierre Lombard, Jérôme Dupeux

Analysis of a Bladed Disk with Friction in Blade Attachments

D. Charleux, C. Gibert, F. Thouverez
Ecole Centrale de Lyon, Laboratoire de Tribologie et de Dynamique des Systèmes, CNRS/UMR 5513
36 avenue Guy de Collongue 69130 ECULLY FRANCE

J.P. Lombard, J. Dupeux
SNECMA Moteurs, Site de Villaroche, 77550 MOISSY CRAMAYEL FRANCE

ABSTRACT

This paper is devoted to the analysis of an experimental bladed disk with contact and friction in the blade roots. The impact of this non linearity on the forced response of the assembly is numerically investigated using a multiharmonic balance method. The full-size finite element model is reduced using a component modes synthesis method and taking centrifugal stiffening into account so as to obtain reduced models of the disk and of the blades. The blade frequency mistuning is measured and introduced in the model. With Coulomb's law of friction, a sensitivity analysis is performed in which the influences of the excitation level and of the rotational speed are studied. The numerical results are compared with the experimental results.

INTRODUCTION

Turbomachine bladed disks are subjected to fluctuating aerodynamic forces. If the resulting vibration is excessive, wear and high cycle fatigue of the blading may be encountered, eventually leading to failure. Therefore, the validation of the design has to include an accurate prediction of the actual vibration levels, especially near the natural frequencies. The forced response of a practical bladed disk is substantially affected by structural damping, aerodynamic damping and friction contacts between its components, but the complex and non linear nature of these mechanisms makes them difficult to model.

Devices with friction dampers are commonly used in bladed disks. Conjointly, the study of their effect on the forced response was the object of numerous papers (see e.g. [1]). Blade root damping however received less attention. Nonetheless some numerical studies revealed that energy dissipation at the blade root could be significant [2][3]. The experimental results of [4] showed that a decrease of the total amount of damping (i.e. sum of material damping and blade root damping) is to be expected as the rotational speed is increased. Sliding distances are small in blade roots and moreover only part of the contact interface may slip. Predicting correctly this microslip requires a good knowledge of the stress distribution over the contact surface. Unfortunately, very fine meshes are necessary to correctly estimate the high stress gradients. This was shown in papers [5][6] where static loading of dovetail attachments is studied. The effect of centrifugal loading on blade root stresses was also investigated in papers [7][8] and the numerical results were confronted with photoelasticity experimental results.

In this paper an experimental bladed disc is studied. It supports four blades through dovetails attachments. The eight root flanks are the contact interfaces retained in the numerical calculations. Since the normal load on the contact surfaces is not known and vary during vibration, microslip models such as the one proposed in [9] are not applicable. On the other hand fine finite elements meshes of the contact interface make the dynamic computations too long. Therefore, a compromise is found and 24 contacts nodes per flank are retained in the numerical investigations. The Dynamic Lagrangian mixed Frequency–Time method (DLFT) [10][2] is used to calculate the harmonic response of the bladed disk with Coulomb's friction and unilateral contact in the blade roots. The confrontation with the experimental results reveals that the numerical method is able to predict the main trends over the rotational speed range studied.

NOMENCLATURE

M, C, K : mass, damping and stiffness matrices
K_c, K_g, K_t : centrifugal, geometrical and tangent stiffness matrices
q : vector of displacements
F_c : vector of contact forces
F_{ex} : vector of external forces
U_a : voltage applied to the piezoelectric ceramic
d_{31} : piezoelectric charge constant of the piezoelectric ceramic
S_1 : area of the cross section of the piezoelectric ceramic
Y_{11} : Young modulus of the piezoelectric ceramic
e : thickness of the piezoelectric ceramic
l_1 : length of the piezoelectric ceramic
K_p : stiffness of the piezoelectric ceramic
K_s : local stiffness of the structure at the location of the piezoelectric ceramic
F_1 : force applied by the piezoelectric actuator on the blade
ξ : material equivalent viscous damping ratio
μ : coefficient of friction

EXPERIMENTAL SETUP

Schematic views of the test bench used can be seen in Fig 1. The rotating disk supports four blades and is placed in a vacuum chamber so as to minimize the effects of aerodynamic forces. The results presented below are obtained with a pressure of 21 mbar. Different rotational speeds can be chosen up to 5000rpm. Two rotating blades are excited by means of piezoelectric devices, which can be seen in Fig 3. The piezoelectric ceramics are insulated from the blades thanks to a special adhesive and were placed on high strains regions of the first bending mode. The two piezo-actuated blades are also equipped with strain gauges. The blade root is linked to the disk via a dovetail type attachment (see Fig 2 b)).

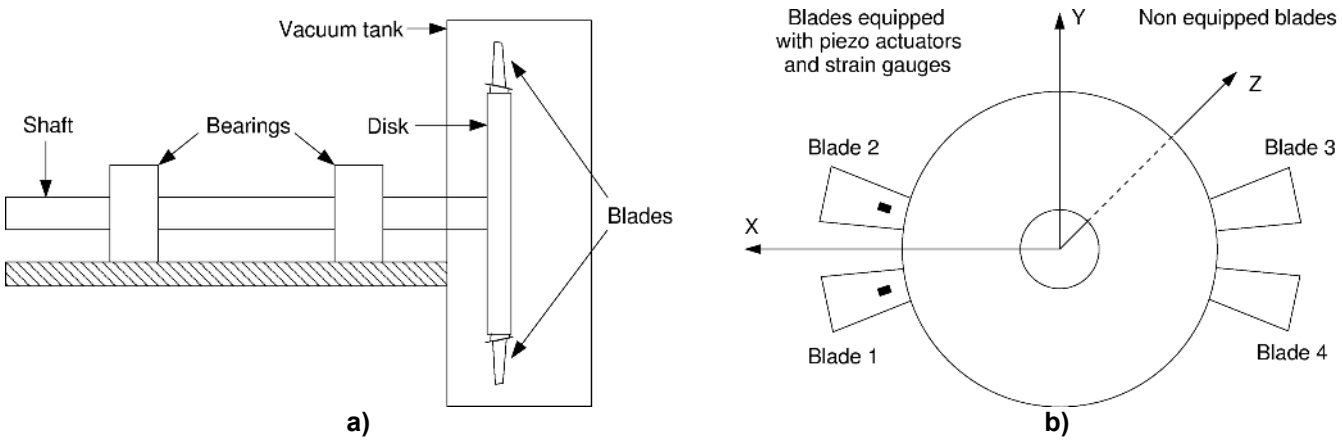

Fig 1. Schematic views of the test bench a) transverse view, b) frontal view.

NUMERICAL MODEL

Finite element model

A numerical model of the bladed disk was created. The four blades and the disk were meshed using second order tetrahedral elements (i.e. 10 nodes per element). The mesh can be seen in Fig 2. The shaft was modeled with beam elements. Rigid body elements were used to link the shaft and the three dimensional mesh of the disk. The two bearings were modeled with axial and radial linear springs.

The commercial FE code Samcef is used to carry out the preliminary linear calculations. The model is divided into five substructures: one for each blade and one for the disk-shaft assembly. The number of degrees of freedom (dofs) is reduced according to the Craig & Bampton component modes synthesis method [11]. The reduced basis of one blade encompasses the dofs of the nodes involved in contact, the dofs necessary to represent the piezo actuators and the strain gauges and three modal dofs. The contact nodes used in the present study can be seen in Fig 2 b). The reduced basis of the disk-shaft assembly encompasses the disk contact nodes and 18 modal dofs. The natural frequencies obtained with the reduced model and those obtained with the full-size model were compared in order to validate the reduced model. At the present stage, rotation is taken into account but the frictional contact non-linearity is not considered: the contact interfaces are assumed to be perfectly welded. Under this assumption the mass matrix M and the tangent stiffness matrix K_t for each substructure are computed and retrieved. The tangent stiffness matrix can be decomposed as

$$K_t = K - K_c + K_g \,, \tag{1}$$

where K is the structural stiffness and K_c is the centrifugal stiffness. The term $-K_c$ is a stiffness correction due to the expression of the equations of motion in the rotating frame and is responsible for a softening effect. K_g is the geometric stiffness matrix which represents the stiffening of the substructure under the rotation-induced stresses. For each substructure, the equations to be solved are written in the reduced basis as

$$M\ddot{q} + C\dot{q} + K_t q + F_c = F_{ex} \,, \tag{2}$$

where F_{ex} stands for the external forces, F_c represents the contact forces and C is a Rayleigh damping matrix. The gyroscopic matrix is not taken into account. Indeed, the results shown in this paper are computed for particular modes of the structure where there is no shaft bending. In this case, it was verified that the forced response computed with the gyroscopic matrix is only very slightly modified. The natural frequencies are shifted by less than 0.01%. These results are in agreement with [12], where using a Ritz method, it was found that the modes of a rotating radial beam were not affected by the Coriolis acceleration.

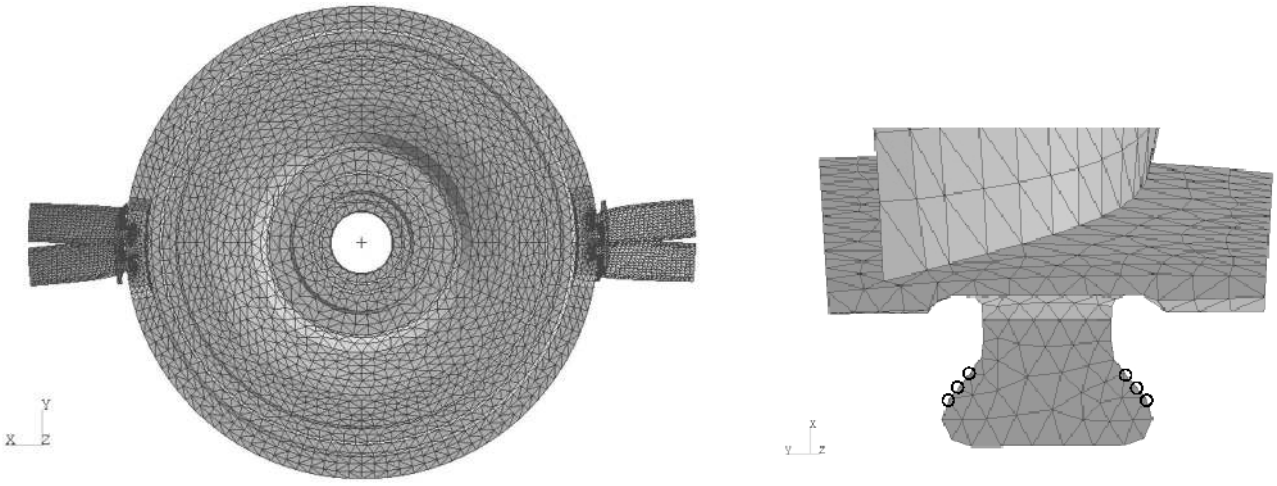

a) **b)**

Fig 2. Numerical model : a) mesh of the disk and the four blades, b) localization of the contact nodes on the blade root : 8x3=24 nodes on each flank.

Frequency mistuning measurement

The word mistuning refers to the small variations of the blade dynamic behavior (natural frequencies and mode shapes). The mistuning between the blades is unavoidable because of manufacturing tolerances and material discrepancies. Furthermore, in the presented experiment, two blades are equipped with excitation and measurement devices, while the two others are not. It is important to include mistuning in the numerical

calculations, since it is known to substantially affect the modes and the forced response of bladed disks [13]. The blades were weighed so as to update the density of each blade finite element model. The frequency mistuning was also measured. A laser vibrometer was used to measure the impulse response of the four blades. The corresponding test bench is shown in Fig 3. As the frequency depends on boundary conditions, the same tightening torque of 10 Nm was imposed in each case to the screw. The reproducibility of the measure was verified. The mean frequencies found are gathered in Table 1. These results suggest a stiffening effect brought by the piezoelectric ceramics. The stiffness updating was carried out considering only the first bending mode of the blade because this mode is dominant in the modes of the whole bladed disk that are studied below. The shaft and disk models were also updated. Impulse responses of the shaft-disk assembly without the blades were measured at rest. The found natural frequencies were used to update the corresponding model. In particular, the bearing spring constants had to be adjusted.

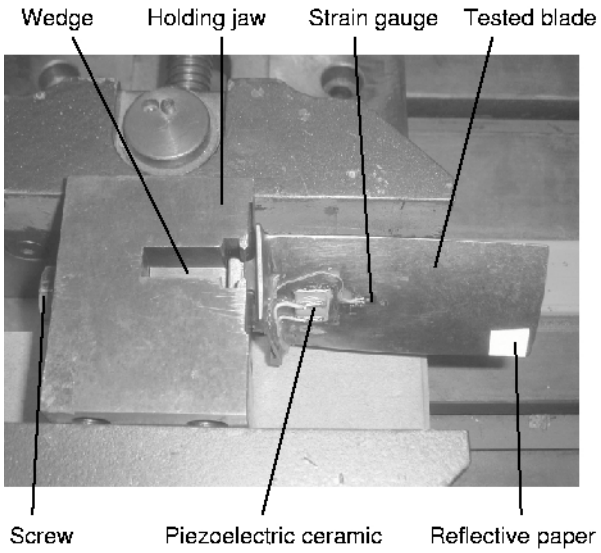

Fig 3. Frequency mistuning measurement with laser vibrometry. Photo of blade 1 : piezo actuators and strain gauges are not used in this test.

	Blade 1	Blade 2	Blade 3	Blade 4
Normalized frequency	0.964	0.972	0.941	0.949
Frequency deviation	+0.8%	+1.6%	-1.6%	-0.8%

Table 1. Measured frequencies of the first bending mode and deviation between each blade frequency and the average frequency

Piezoelectric excitation modeling

The piezoelectric actuators are modeled with the simple unidirectional model shown in Fig 4. The load is assumed to be transmitted to the structure via the two extremes points A and B. The force produced by the actuator when a voltage U_a is applied to the electrodes can be written as [14]

$$F_1 = \frac{Y_{11} S_1}{l_1} \Delta l_1 - \frac{d_{31} S_1 Y_{11}}{e} U_a, \tag{3}$$

where d_{31} is the piezoelectric charge constant of the ceramic, S_1 is the area of the cross section, Y_{11} is the Young modulus of the ceramic in direction 1. e, l_1 and Δl_1 are respectively the thickness of the ceramic, the length of the ceramic and the elongation in direction 1. The stiffness of the piezo actuator between points A and B is denoted K_p :

$$K_p = \frac{Y_{11} S_1}{l_1}. \tag{4}$$

If K_s is the local stiffness of the structure in direction 1 at the location of the actuator, then F_1 can also be expressed as

$$F_1 = -K_s \Delta l_1. \tag{5}$$

Combining equations (3),(4) and (5), a simple expression of the excitation force as a function of the applied voltage is obtained :

$$F_1 = -\frac{d_{31} S_1 Y_{11}}{e\left(1 + \frac{K_p}{K_s}\right)} U_a. \tag{6}$$

Each blade is equipped with two actuators (i.e. one on each side of the airfoil) fed by out of phase sinusoidal voltages. It is necessary to keep 2 nodes per actuator in the reduced basis in order to use the proposed model.

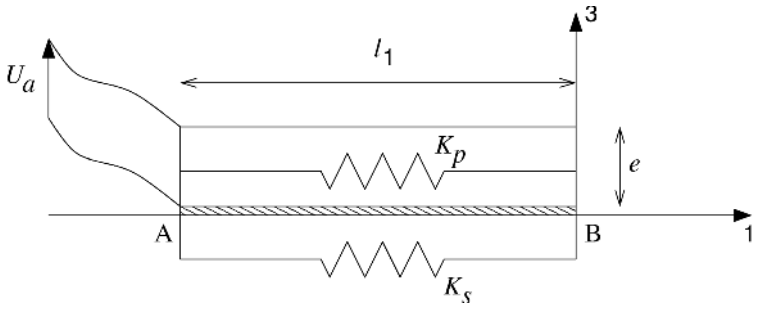

Fig 4. Model of piezoelectric excitation.

Nonlinear analysis

The steady-state solutions of equations with contact forces (2) are sought with the Dynamic Lagrangian mixed Frequency–Time method (DLFT) [10][2]. This is a multiharmonic balance method. The non linear problem is formulated in the frequency domain and the contact forces are computed in the time domain with a prediction-correction method [2]. One important feature of the DLFT is the ability to take into account directly the laws of unilateral contact and Coulomb friction. It is not necessary to smooth them or to introduce normal and tangential contact springs. Three dimensional node-to-node contact elements are used. They take into account the variable normal load at the blade root and the 2D stick-slip motion. In the present study, there are 192 contact elements which represents 384 contact nodes and 1152 nonlinear degrees of freedom. With the linear dofs added, the total size of the problem is 1290. The size of the system to be solved by the nonlinear solver is actually 576. This is achieved by performing two exact reductions in the frequency domain. In the first one, only the 1152 degrees of freedom involved in the contact elements are retained. Further factor two reduction is obtained by writing the problem in terms of relative displacements. The computations are performed in two steps. The first step is the determination of the sliding displacement in the blade root due to the centrifugal load. The found position is then used as a starting point for the calculation of the forced response.

RESULTS

The experimental and numerical forced responses presented in this section were obtained by analyzing a narrow excitation frequency range which includes 2 resonance peaks. For this two resonant modes, the strain energy is mainly localized in a single blade which vibrates according to its first bending mode. In mode 1, blade 1 has the

greatest vibration amplitude among the four blades whereas the amplitude of blade 2 is much lower and blade 1 and 2 vibrate in phase. In mode 2, vibration is mainly localized in blade 2 with blade 1 and 2 vibrating out of phase. The excitation was applied to blade 2 only.

Fig 5 shows the experimental and numerical harmonic responses for 4 different levels of excitation. The numerical responses were obtained with a friction coefficient of μ = 0.08 and an equivalent viscous damping ratio ξ = 0.075 % due to material damping. This damping ratio is defined by the linear case were all the contact elements are stuck (i.e. no energy dissipation due to friction). ξ is assumed to be independent of the strain amplitude and of the rotational speed. The values of ξ *and* μ were chosen so as correctly represent the total amount of damping over the rotational speed range. Under these assumptions, Fig 5. shows a good agreement between experimental and numerical results. A small frequency shift of 0.2% is noticed when U_a is increased from 10V to 80V, which is not exactly reproduced by the simulation. The phase diagrams of Fig 5 should be seen bearing in mind that the strain gauge of blade 1 is mounted on the suction side of the airfoil and that the strain gauge of blade 2 is mounted on the pressure side. Therefore, mode 1 is effectively an in phase mode and mode 2 an out of phase mode.

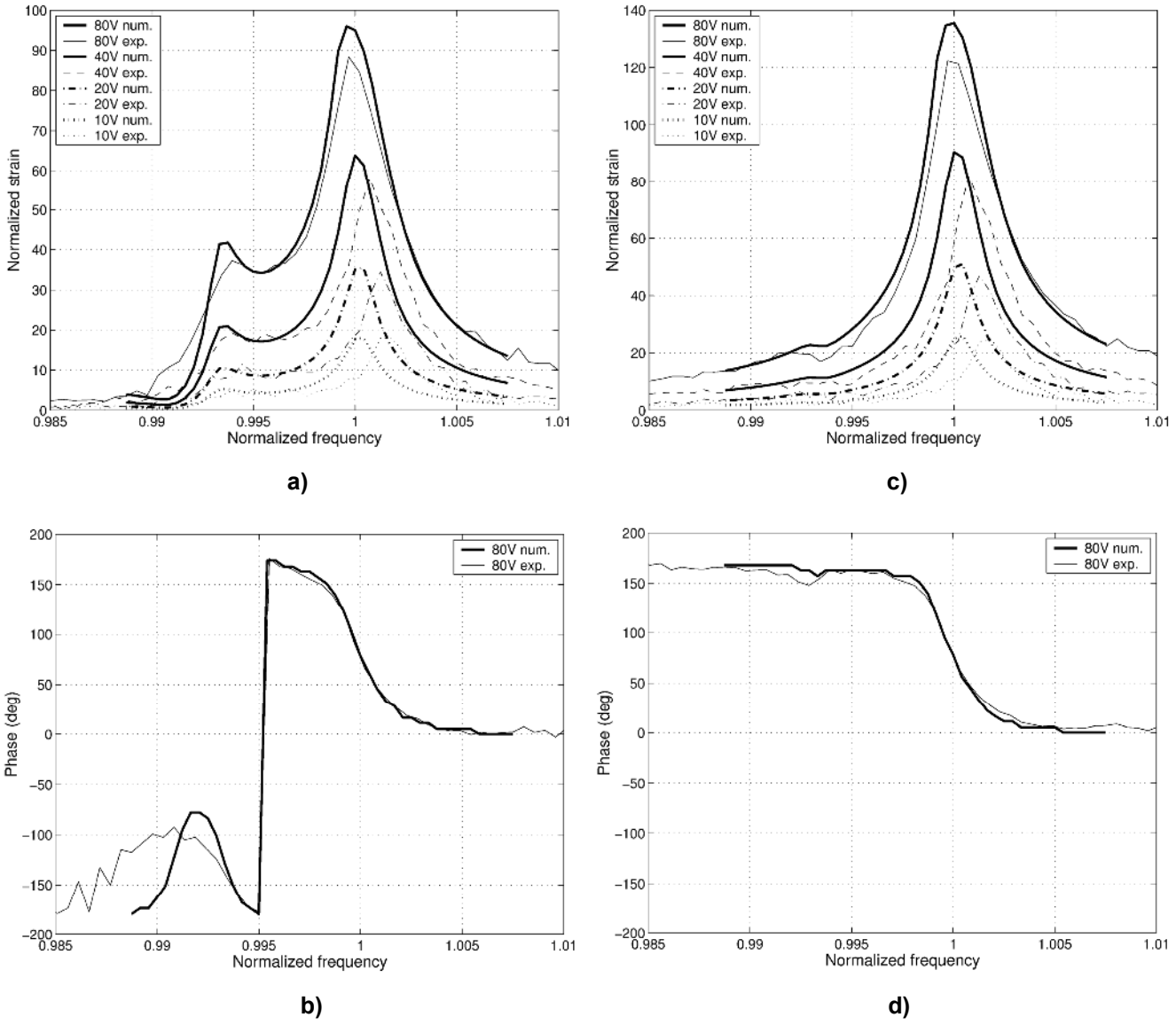

Fig 5. Numerical and experimental forced responses at Ω=3000 rpm : a) vibration level of blade 1, b) phase of blade 1, c) vibration level of blade 2, d) phase of blade 2.

The numerical results of Fig 5 were computed with one harmonic. The influence of the number of harmonics retained is presented in Fig 6 b). Retaining more than 3 harmonics does not seem to improve the convergence. A maximum discrepancy of 5% is found between the results obtained with 1 harmonic and 5 harmonics. Fig 6 a) shows how blade root friction affect the harmonic response. In this case, the maximum vibration level is found to be noticeably lower than when friction is not considered.

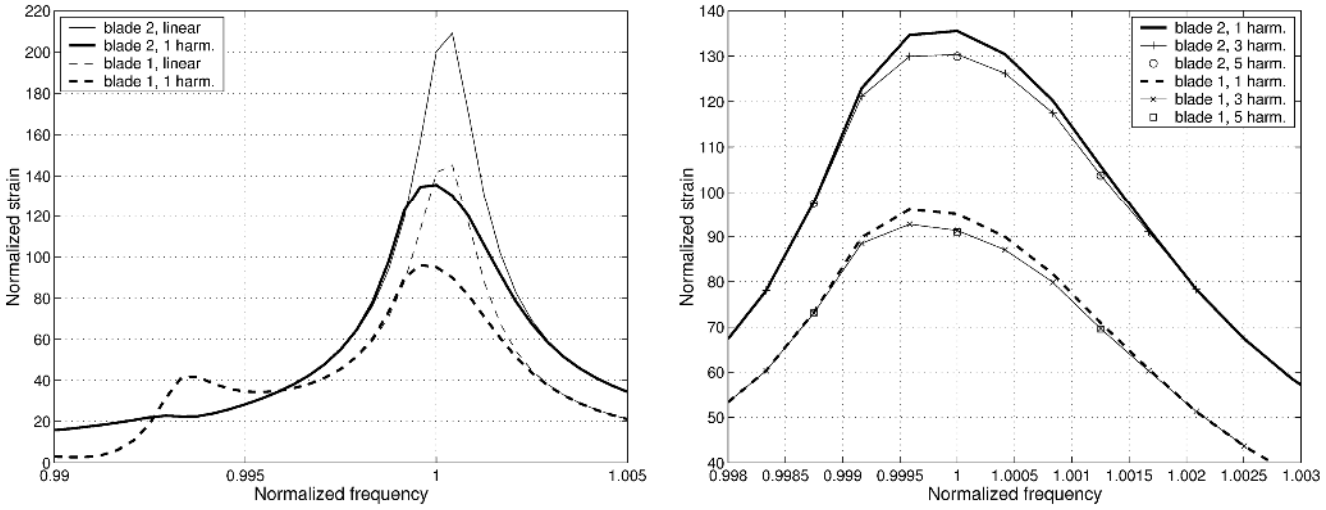

a) **b)**

Fig 6. Numerical forced responses with Ω=3000 rpm and U_a=80V: a) comparison between the all stuck case (linear) and the stick-slip case , b) effects of the number of harmonics retained.

The experiments and the computations were carried out at 4 rotational speeds : 2000, 3000, 4000 and 5000 rpm. Fig 7 shows the evolution of the resonant frequency for mode 2 over the speed range. This result is obtained with a low excitation level so as to minimize the frequency shift due to the nonlinearity. The numerically predicted centrifugal stiffening is in close agreement with the experiment. The maximum measured and numerical strains are plotted as a function of rotational speed in Fig 8 and Fig 9 shows the corresponding equivalent viscous damping. Energy dissipation is shown to increase with the level of excitation both in experiments and computations.

It is interesting to discuss the results obtained for the two extremes spinning speeds, i.e. 2000 rpm and 5000 rpm. Fig 9 a) shows that the total amount of damping predicted by the simulation at 2000 rpm is overestimated for the maximum excitation level. This is a case where frictional damping is predominant over material damping. This suggests that the friction coefficient value used in the computations may be too low. The value μ = 0.08 indeed seems low, even if the blade roots are covered with a solid lubricant. The computations carried out at 5000 rpm revealed that only few contact elements were sliding and with a very low amplitude, which means that there is almost no amplitude reduction due to friction. This suggests the material damping in the computations (ξ = 0.075 %) may be overestimated since the computed strains are lower than the measured strains.

The previous observations lead us to discuss the validity of some assumptions made in the proposed numerical model. Each contact interface is modeled with 24 contact elements. References [5] [6] show that a much finer discretization is required to accurately predict the stress distribution. This means that there is probably a difference between the predicted localization of the sliding dissipation and the real one. Microslip and the energy dissipations associated with it are difficult to model. Maybe the friction law used should be more precise for small sliding distances and velocities.

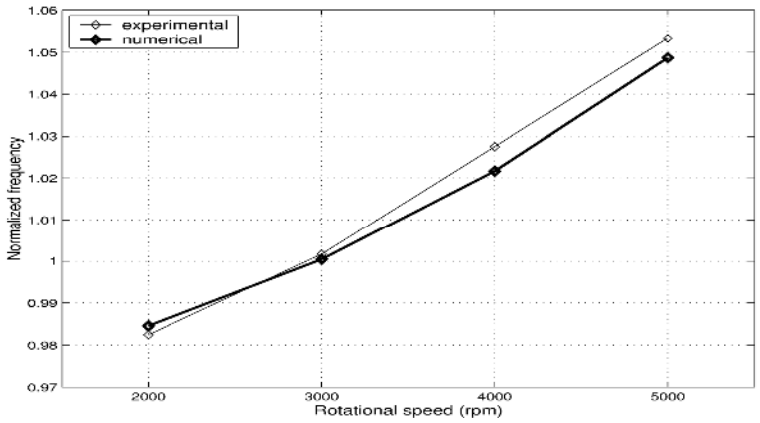

Fig 7. Numerical and experimental resonant frequencies for U_a=10V.

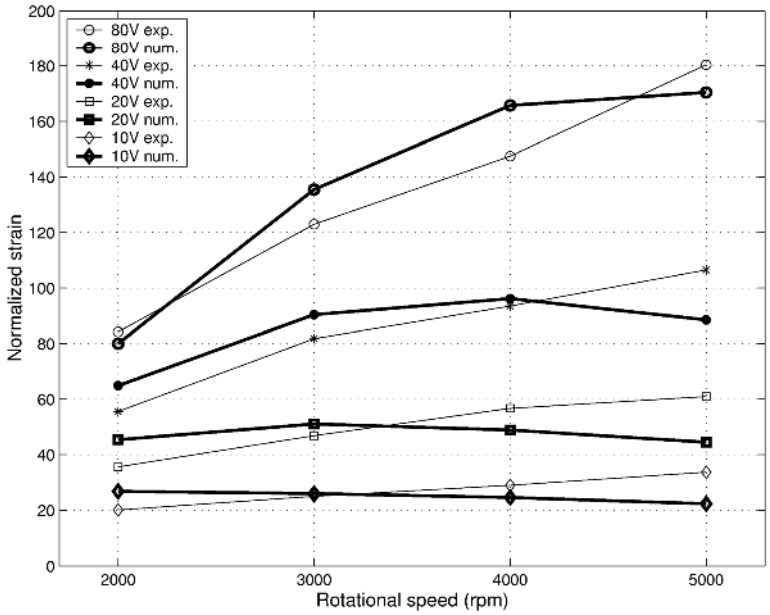

Fig 8. Numerical and experimental maximum vibration levels of blade 2.

CONCLUSION

The effect of blade root friction on the forced response of bladed disks was investigated both numerically and experimentally. A complete model of the test bench was built. Its size was reduced with the Craig & Bampton component modes synthesis method. Centrifugal stiffening and blade mistuning were taken into account. The friction contact problem is solved in the frequency domain with an efficient multiharmonic balance method.

A sensitivity analysis was performed where the excitation level and the rotational speed were varied. The numerical and experimental results were systematically compared. The numerical model was shown to reproduce the main trends. Some possible causes of the remaining deviations were discussed.

ACKNOWLEDGMENTS

We are pleased to acknowledge the technical and financial support of this work by SNECMA Moteurs.

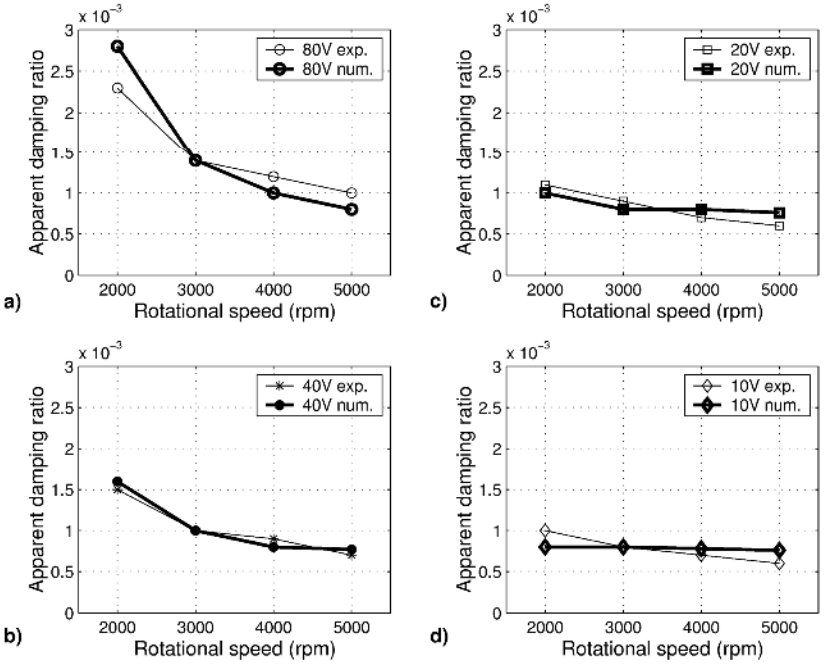

Fig 9. Numerical and experimental equivalent viscous damping ratio.

REFERENCES

[1] Berthillier M., Dupont C., Mondal R., Barrau J.J., *Blades forced response analysis with friction dampers*, Journal of Vibration and Acoustics, vol 120, pp 468-474, 1998.

[2] Charleux D., Thouverez F., Lombard J.P., *Three-dimensional multiharmonic analysis of contact and friction in dovetail joints*, IMAC XXII, January 2004, Dearborn, Michigan, paper 348.

[3] Petrov E.P., Ewins, D.J., *Analysis of essentially non-linear vibration of large-scale models for bladed discs with variable contact and friction at root joints*, 8th International Conference on Vibrations in Rotating Machinery, September 2004, Swansea, UK, pp163-172.

[4] Rao J.S., Usmani M.A.W., Ramakrishnan C.V., *Interface damping in blade attachment region*, 3rd International Conference on Rotor Dynamics, September 1990, Lyon, France, pp 185-190.

[5] Beisheim J.R., Sinclair G.B., *On the three-dimensional finite element analysis of dovetail attachments*, Journal of Turbomachinery; vol 125, pp 372-379, 2003.

[6] Sinclair G.B., Cormier N.G., Griffin J.H., Meda G., *Contact stresses in dovetail attachments: finite element modeling*, Journal of Engineering for Gas Turbines and Power, vol 124, pp 182-189, 2002.

[7] Meguid S.A., Kanth P.S., Czekanski A., *Finite element analysis of fir-tree region in turbine discs*, Finite Elements in Analysis and design, vol 35, pp 305-317, 2000.

[8] Papanikos P., Meguid S.A., Stjepanovic Z., *Three-dimensional nonlinear finite element analysis of dovetail joints in aeroengine discs,* Finite Elements in Analysis and Design, vol 29, pp 173-186, 1998.

[9] Menq C.H., Bielak J., Griffin J.H., *The influence of microslip on vibratory response, part i : a new microslip model*, Journal of Sound and Vibration, vol 107, no 2, pp 279-293, 1986.

[10] Nacivet S., Pierre C., Thouverez F., Jezequel L., *A dynamic Lagrangian frequency-time method for the vibration of dry-friction-damped systems,* Journal of Sound and Vibration, vol 265, no 1, pp 201-219, 2003.

[11] Craig R.R., Bampton M.C.C., *Coupling of substructures for dynamic analysis*, AIAA Journal, vol 6, no 7, pp 1313-1319, 1968.

[12] Laurenson R.M., *Modal analysis of rotating flexible structures*, AIAA Journal, vol 14, no 10, pp 1444-1450, 1976

[13] Seinturier E., Lombard J.P., Berthillier M., Sgarzi O., *Turbine mistuned forced response prediction, Comparison with experimental results*, ASME Turbo Expo, June 2002, Amsterdam, The Netherlands, paper GT-2002-30424.

[14] Jemai B., *Contrôle actif de structures flexibles à l'aide de matériaux piezo-électriques : applications*, PhD thesis, Ecole Centrale de Lyon, France, 1999.